Thin Solid Films 519 (2011) 3312–3317

Contents lists available at ScienceDirect

Thin Solid Films

journal homepage: www.elsevier.com/locate/tsf

Intrinsic room temperature ferromagnetism in $Zn_{0.92}Co_{0.08}O$ thin films prepared by pulsed laser deposition

Hanbin Wang [a], Qiong He [a], Hao Wang [a,*], Xina Wang [a], Jun Zhang [a,*], Yong Jiang [b], Quan Li [c]

[a] Faculty of Physics and Electronic Technology, Hubei University, Wuhan 430062, PR China
[b] School of Materials Science and Engineering, University of Science and Technology Beijing, Beijing 100083, China
[c] Department of Physics, Chinese University of Hong Kong, Hong Kong, China

ARTICLE INFO

Article history:
Received 29 January 2010
Received in revised form 23 December 2010
Accepted 4 January 2011

Keywords:
Diluted magnetic semiconductors
Zinc oxide
Co-doping
Magnetic properties
Defects
X-ray absorption fine structure
X-ray diffraction
Scanning electron microscopy

ABSTRACT

$Zn_{0.92}Co_{0.08}O$ thin films were fabricated on *p*-type Si (100) and quartz substrates by pulsed laser deposition using a ZnCoO ceramic target. The structural and magnetic properties of the films were characterized by field emission scan electronic microscopy, x-ray diffraction, x-ray photoemission spectroscopy, UV-visible transmission spectra, extended x-ray absorption fine structure spectroscopy and physical property measurement system. Substitutional doping of Co^{2+} in ZnO lattice is demonstrated in the films. The as-deposited $Zn_{0.92}Co_{0.08}O$ thin film displayed intrinsic room temperature ferromagnetism with saturation magnetization (M_s) of ~0.20μ_B/Co. The corresponding M_s increased to ~0.23μ_B/Co when annealed in vacuum and further to ~0.42μ_B/Co after annealed in hydrogen. In turn, the M_s dropped to the value of ~0.13μ_B/Co after annealed in oxygen. Our studies indicate that oxygen vacancy density plays a key role in mediating the ferromagnetism of the diluted magnetic semiconductor films.

1. Introduction

Diluted magnetic semiconductors (DMSs) have attracted much attention due to their unique spintronic properties with potential technological applications [1–4]. Among numerous DMSs, the 3d transition metal (TM) doped ZnO have been intensively studied not only because of their desired high curie temperature predicted by theoretical and experimental studies, but also abundance in nature, controllable synthesis as well as the outstanding transport properties [1, 3, 5, 6]. Up to date, room temperature ferromagnetism of ZnO-based DMS materials has been reported by many groups [7–9]. Recently, Wang et al. reported the room temperature ferromagnetism for the Co-doped ZnO films prepared by electrochemical deposition [10]. Xu et al. reported single-phase $Zn_{1-x}Co_xO$ (x = 0.02, 0.04) powders synthesized by a simple co-precipitation technique showing robust room temperature ferromagnetic behavior [11]. Though ferromagnetism was extensively observed in the Co:ZnO films and nanostructures, there have been some reports which argued that the Co:ZnO itself is non-ferromagnetic [12–14] and the experimentally observed ferromagnetism in Co:ZnO films comes from the secondary magnetic phases such as $ZnCo_2O_4$ or Co clusters [15, 16]. To clarify the origin of the magnetic properties of DMSs, various magnetic interaction mechanisms based on carrier-mediated ferromagnetism [3, 17], the *sp-d* exchange, and the double exchange between *d* states of TM elements have been proposed [1]. On the other hand, defects related to magnetic exchanges have been suggested to play an important role in the magnetic origin for oxide DMSs. Different mechanisms such as structural defects, oxygen vacancy, Zn interstitials, Zn vacancies have been proposed to be responsible for the occurrence of ferromagnetism in ZnO based DMSs [18, 19]. The real role of defects in mediating ferromagnetic ordering still remains unclear at present [20, 21]. To clarify the origin of the ferromagnetism in the ZnO-based DMSs, experimental investigations based on different methodologies are particularly in need.

In this work, pulsed laser deposition (PLD) was used to deposit Co-doped ZnO thin films on *p*-type Si (100) and quartz substrates. The effect of annealing atmosphere on the structure and magnetic properties of the $Zn_{0.92}Co_{0.08}O$ thin films was investigated. After annealed in oxygen, the saturation magnetic moment (M_s) of the $Zn_{0.92}Co_{0.08}O$ thin films decreases 35% compared with the as-deposited thin film, while the corresponding value increases 15% and 110% after annealed in vacuum and hydrogen respectively. The observations suggest that the defect (oxygen vacancy) mediated exchange mechanism is responsible for ferromagnetic ordering in the Co:ZnO films.

* Corresponding authors. Fax: +86 27 88663390.
E-mail addresses: nanoguy@126.com (H. Wang), gwen_zhang1102@hotmail.com (J. Zhang).

0040-6090/$ – see front matter © 2011 Elsevier B.V. All rights reserved.
doi:10.1016/j.tsf.2011.01.090

2. Experiment

In the experiments, $Zn_{0.92}Co_{0.08}O$ thin films were deposited on *p*-type Si (100) and quartz glass substrates by a PLD technique. The content of Co in ZnO thin films was measured by x-ray fluorescence. The films grown on quartz substrate were characterized by UV–visible transmission spectroscopy and Hall effect sensor. The ceramic target of ZnCoO was prepared by conventional solid-state reaction method. Well mixed stoichiometric mixtures of 4 N purity ZnO and Co_2O_3 powders were calcined at 873 K for 10 h in the air with an intermediate regrinding. The obtained powder was ground, pelletized, and sintered at 1473 K for 10 h in the air, then the sintered target was cooled down to room temperature naturally. A pulsed KrF excimer laser ($\lambda = 248$ nm and $\tau = 25$ ns) was used for the ablation of the target. Prior to deposition, the Si substrates were dipped into 10% HF solution for 30 s to remove native oxide and then cleaned sequentially with acetone, anhydrous alcohol and deionized water. The substrates were placed at a distance of 50 mm away from the target. Before deposition, the target was pre-ablated for 15 min to remove surface contamination, while a shutter was put to prevent the substrate from being deposited. The target and the substrate holder are kept rotating during the process of the film growth in order to obtain a uniform deposition. The energy density and the repetition rate of the laser beam were 250 mJ/pulse and 10 Hz, respectively. The deposition chamber was evacuated to a base pressure of $\sim 10^{-4}$ Pa. During the deposition, the substrate temperature was kept at 873 K and the deposition period was 3 h, yielding films with thickness of about 500 nm. In order to study the effects of defects (oxygen vacancies) on magnetism, some of the as-deposited films were post-annealed in oxygen/hydrogen atmospheres of 20 Pa and vacuum at 973 K for 100 min, respectively.

The structure of $Zn_{0.92}Co_{0.08}O$ films was characterized by x-ray diffractometer (XRD, Bruker D8) with Cu Kα radiation and Ni filter. The morphology of the thin films was investigated by field emission scanning electronic microscopy with operating voltage of 20 kV. (FE-SEM, JEOL JSM-6700F). The bonding states of cobalt and oxygen elements in samples were examined by x-ray photoemission spectroscopy (XPS) using Al Kα radiation ($h\upsilon = 1486.6$ eV). The samples were cleaned by Ar ion sputtering with 3 keV energy and current density of 5 μA cm^{-2}. The binding energy was measured with respect to C 1s peak of adventitious carbon (248.5 eV). The peaks for Co $2p_{3/2}$ and $2p_{1/2}$ and their shakeups are fitted using a mixed method of Gaussian and Lorentzian functions by using software (XPS Peak 4.1). The room temperature UV–visible transmission spectra were measured in the range of 200–800 nm using an UV–vis–NIR spectrophotometer. The Co *K*-edge extended x-ray absorption fine structure (EXAFS) measurements were carried out at the XAFS station in the National Synchrotron Radiation Laboratory (NSRL) of University of Science and Technology of China. The data of $Zn_{0.92}Co_{0.08}O$ were collected in fluorescence mode, and the reference data from Co foil, CoO, Co_2O_3, and ZnO powders were collected in transmission mode at room temperature. The magnetic properties were measured using a physical property measurement system (PPMS) in the temperature range of 10–350 K, with a magnetic field parallel to the film plane and all of the magnetization data have been corrected for the diamagnetic contribution of the Si substrates. Room temperature Hall effect measurements were performed on Accent HL5500 Hall System using four-point van der Pauw-Hall method.

3. Results and discussion

XRD patterns of ZnCoO target as well as the corresponding as-deposited, O_2-annealed, vacuum-annealed and H_2-annealed $Zn_{0.92}Co_{0.08}O$ thin films are shown in Fig. 1a and b, respectively. The polycrystalline XRD pattern in Fig. 1a suggests that the target is single phase with a hexagonal ZnO wurtzite structure and no traces of any secondary phase or metal-related peaks are observed. In addition, as shown in Fig. 1b, the four samples show similar hexagonal ZnO wurtzite structure XRD patterns. The ZnO (002) diffraction peak is predominant in the patterns indicating that the crystals are with preferential growth direction along $(002)_{ZnO}$ in the films. The weakness of the (103), (200), (112) diffraction peaks indicate that the alignment along $(002)_{ZnO}$ of the films are improved after annealed in vacuum and oxygen atmospheres, especially in the oxygen atmosphere. But the phenomenon is not obvious for the H_2-annealed sample. On the other hand, as marked on the X-axes of Fig. 1b, no diffraction peaks related to cobalt oxides were observed in the O_2-annealed sample, nor diffraction peak of metallic cobalt was presented in vacuum/H_2-annealed (reducing atmosphere) samples. These facts suggest the lack of secondary phase in the as-deposited $Zn_{0.92}Co_{0.08}O$ thin films. Then, the XRD analysis indicates that Co-doping and post-annealing do not change the ZnO crystallography structure and the cobalt atoms are fully incorporated into the ZnO lattice within the detection limits of this technique.

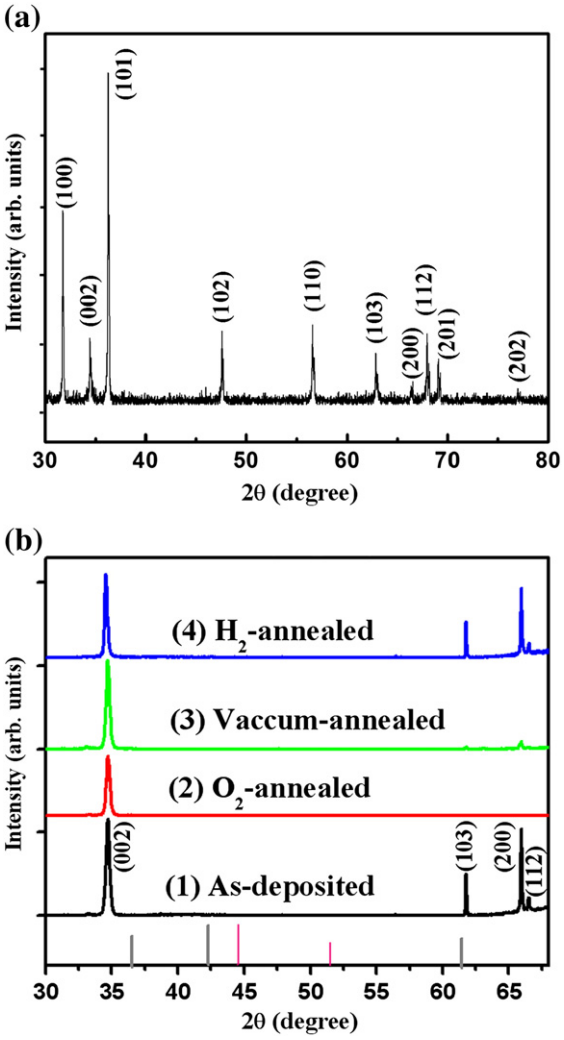

Fig. 1. θ–2θ XRD patterns of the (a) $Zn_{0.92}Co_{0.08}O$ target and (b) $Zn_{0.92}Co_{0.08}O$ thin films deposited on Si (100) substrates: (1) as-deposited, (2) O_2-annealed, (3) vacuum-annealed, and (4) H_2-annealed. The diffraction peaks of metallic Co (pink) and CoO (gray) are marked on the X-axes of (b) for comparison.

Fig. 2 presents the FE-SEM images of as-deposited, vacuum-annealed, O_2-annealed and H_2-annealed $Zn_{0.92}Co_{0.08}O$ thin films, respectively. It can be seen from Fig. 2a that the as-deposited film possesses piece-like crystals. After vacuum-annealing, the film is

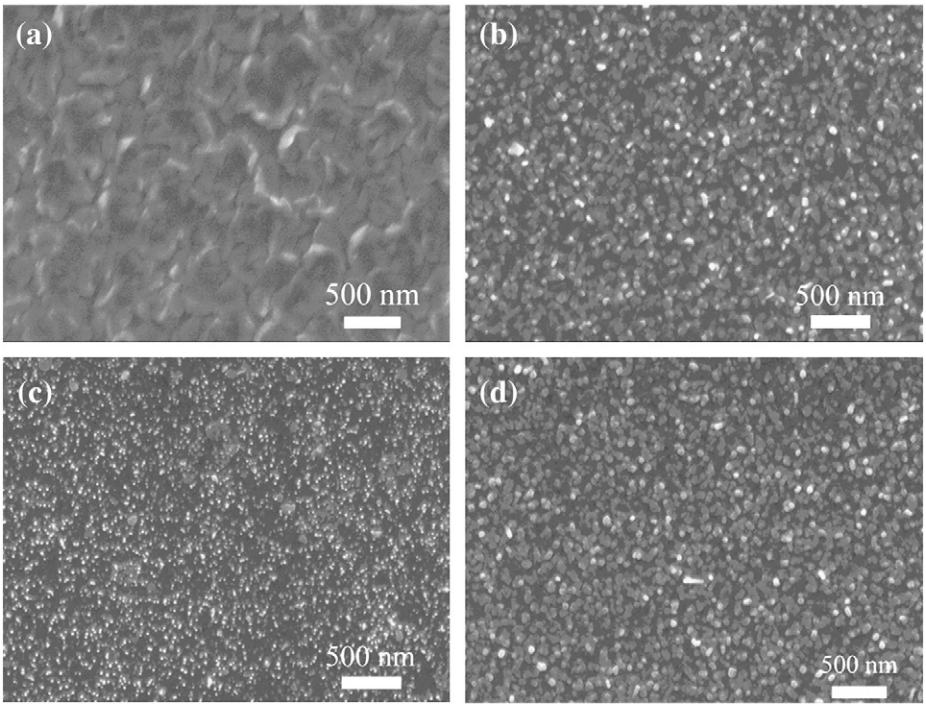

Fig. 2. FE-SEM images of $Zn_{0.92}Co_{0.08}O$ thin films deposited on Si (100) substrates: (a) as-deposited, (b) vacuum-annealed, (c) O_2-annealed, and (d) H_2-annealed.

found to be composed of densely packed uniform columnar crystals (Fig. 2b). After annealed in oxygen atmosphere and hydrogen atmosphere, the size distribution of crystals in the films is homogenous as well (Fig. 2c and d). The results suggest that high temperature annealing improve the uniformity of the crystals in $Zn_{0.92}Co_{0.08}O$ thin films.

XPS was used to investigate the bonding characteristics and oxidation states of the dopant atoms in the as-deposited $Zn_{0.92}Co_{0.08}O$ film. Fig. 3a shows the high resolution scan XPS spectrum of the Zn $2p_{3/2}$ peak which locates at 1021.9 eV. The highly symmetry of the peak indicates that Zn exists in the +2 state within the $Zn_{0.92}Co_{0.08}O$ film. The high resolution scan XPS spectrum of the Co 2*p* peak of the as-deposited sample is shown in Fig. 3b. The Co $2p_{3/2}$ and $2p_{1/2}$ core levels for Co dopants are found to be at 781.4 eV and 796.9 eV with clear satellite peaks located at 786.5 eV and 802.7 eV, respectively, being in agreement with that of Co in an oxygen surrounded environment [22]. As it has been known, if Co exists as metal clusters (Co^0) itself in the film, the bonding energy should be 778.3 eV for the Co $2p_{3/2}$ peak and the energy difference between Co $2p_{3/2}$ and $2p_{1/2}$ core levels is 14.97 eV [23]. The high resolution scan XPS spectrum of the Co 2*p* shown in Fig. 3b confirms that Co exists in the +2 formal oxidation state in tetrahedral symmetry and excludes the possibility of forming Co-metal clusters. Fig. 3c is a typical O 1s XPS high resolution scan spectrum of as-deposited film. It was observed that the O 1s peak can be de-convoluted into two components. The peak at ~530 eV can be ascribed to O^{2-} ions in a wurtzite structure of hexagonal Zn^{2+} ion arrays, whereas the peak at ~532 eV is related with O^{2-} ions in oxygen-deficient regions [23]. It suggests that there are a large number of oxygen vacancy defects in the as-deposited $Zn_{0.92}Co_{0.08}O$ thin film.

The room temperature UV–visible transmission spectra for the as-deposited and H_2-annealed $Zn_{0.92}Co_{0.08}O$ thin films are shown in Fig. 4. The spectra show characteristic absorption peaks approximately located at 568, 616, and 658 nm wavelengths. These peaks are characteristics of *d*–*d* transitions of the tetrahedrally coordinated high-spin state Co^{2+} ions. They are assigned to the $^4A_2(F)$–$^2E(G)$, $^4A_2(F)$ –$^4T_1(P)$, and $^4A_2(F)$ –$^2A_1(G)$ transitions, respectively [24, 25]. The presence of the sub-band transitions indicate that the Co^{2+} ions have substituted for Zn^{2+} ions in a tetrahedral crystal field without changing the wurtzite crystal structure of ZnO in the Co:ZnO films.

In order to further exclude the existence of Co-related secondary phases, the normalized near-edge spectra of EXAFS at the Co *K*-edge of as-deposited, H_2-annealed $Zn_{0.92}Co_{0.08}O$ films and reference samples of Co, CoO, and Co_2O_3 and the Zn *K*-edge of ZnO are presented in Fig. 5a. One can see that the shoulders, main peaks and shapes of $Zn_{0.92}Co_{0.08}O$ films are different from those of CoO, Co_2O_3, and Co foil. The difference in the positions of absorption edge excludes the existence of Co_2O_3. Specifically, in the region of 7737 eV ($E–E_{edge} = 28$ eV) where there is a decrease in intensity for the CoO spectrum as well as an increase in intensity for the $Zn_{0.92}Co_{0.08}O$ films indicate the films do not contain CoO [26]. Besides, the Co *K*-edge spectra of the samples show clear 1s-3d pre-edge absorption peaks which locate at around 7709 eV ($E–E_{edge} = 0$ eV), in contrast to the typical shoulder around 7712 eV ($E–E_{edge} = 3$ eV) for Co foil. These features are characteristic of Co^{2+} dissolve into ZnO and substitute for Zn^{2+} ions in the valence of +2 state [27]. Fig. 5b shows the Fourier transforms (radial distribution functions, RDFs) of the Co *K*-edge EXAFS oscillation functions $k^3X(k)$ for as-deposited and H_2-annealed $Zn_{0.92}Co_{0.08}O$ thin films. The Co *K*-edge functions for Co foil, CoO and Co_2O_3 powders, Zn *K*-edge for ZnO are also shown as references. The first and second major peaks in the RDFs of the pure ZnO correspond to the nearest O and Zn atoms from the central Zn atoms. For $Zn_{0.92}Co_{0.08}O$ samples, they correspond to the nearest O and Zn atoms from the central Co atom. Fig. 5b shows that the RDF shapes of $Zn_{0.92}Co_{0.08}O$ films are similar to that of ZnO but they are significantly different from Co, CoO and Co_2O_3. The interatomic distances for both two major peaks (1.55 and 2.86 Å) of $Zn_{0.92}Co_{0.08}O$ are close to those of ZnO (1.56 and 2.87 Å) rather than Co-related metal or oxides. It is therefore excluded the existence of Co cluster or Co-related secondary phase. Clearly, the aforementioned results of XRD patterns, XPS spectra, UV-visible transmission spectra as well as EXAFS give strong evidence that the doped Co ions are located substitutionally at the Zn sites for the as-deposited and annealed $Zn_{0.92}Co_{0.08}O$ thin films.

Up to date, several different mechanisms have been proposed to explain the ferromagnetic property of DMSs, among which defect (oxygen vacancy)-mediated mechanism has been extensively

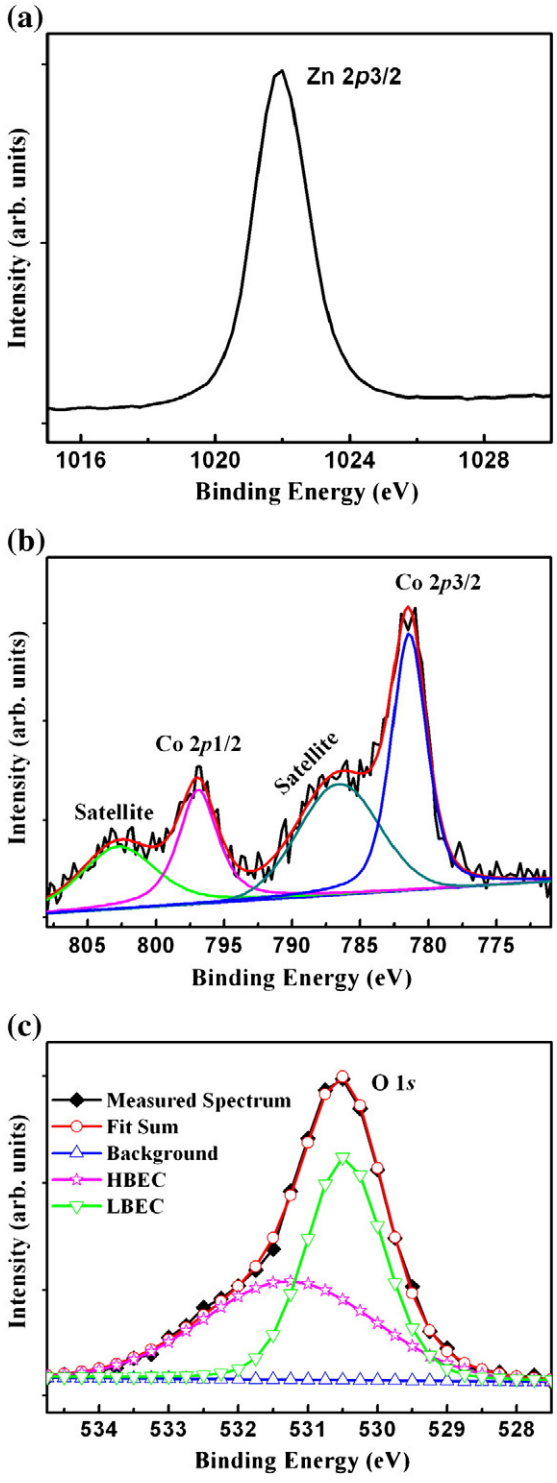

Fig. 3. XPS high-resolution scan spectra of (a) Zn 2*p*, (b) Co 2*p*, and (c) O 1s peaks for as-deposited $Zn_{0.92}Co_{0.08}O$ thin film deposited on Si (100) substrate.

discussed. The relationship between oxygen vacancy concentration and ferromagnetic ordering has been recently reported on some DMSs systems, such as Fe:SnO_2 [28], Co:TiO_2 [29], Co:CeO_2 [30], Co:ZnO [31–34], Ni:ZnO [35] and Mn:ZnO [36]. Based on this, considering that the Zn0.92Co0.08O thin films were deposited under vacuum environment, a large number of oxygen vacancies might be generated in the as-deposited films, which has been demonstrated by the XPS results discussed earlier. On the other hand, oxygen is an effective oxidant to decrease the density of oxygen vacancies in DMS films during

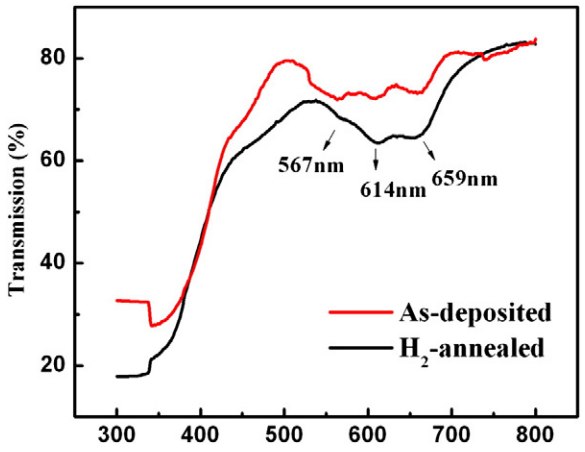

Fig. 4. Room temperature optical transmission spectra of the (a) as-deposited and (b) H_2-annealed $Zn_{0.92}Co_{0.08}O$ thin films deposited on quartz substrates.

annealing process, while hydrogen as an effective reducer will create more oxygen vacancies. In our experiment, post-annealing the $Zn_{0.92}Co_{0.08}O$ films was applied respectively in oxygen, vacuum and

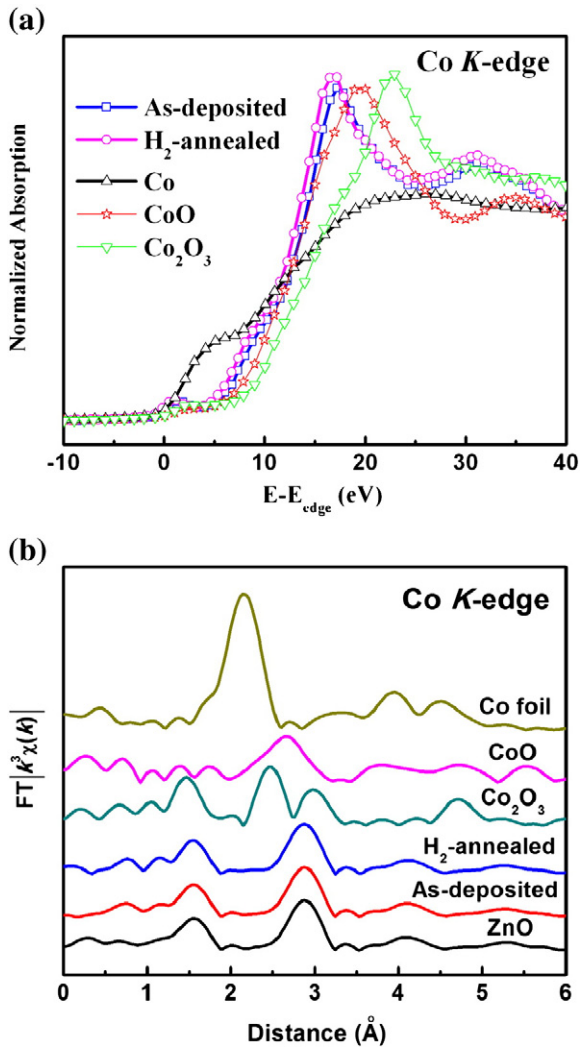

Fig. 5. (a) The normalized near-edge spectra of EXAFS at Co *K*-edge for as-deposited and H_2-annealed $Zn_{0.92}Co_{0.08}O$ thin films and reference samples of Co foil, CoO, and Co_2O_3 powders. (b) Fourier transforms at the Co *K*-edge of k^3-weighted EXAFS oscillation functions for as-deposited and H_2-annealed $Zn_{0.92}Co_{0.08}O$ thin films, respectively. Zn *K*-edge for ZnO powder is also shown for reference.

hydrogen atmospheres to investigate the influence of oxygen vacancy density on the magnetic properties and accordingly interpret the origin of the room temperature ferromagnetism. Fig. 6a presents the magnetization-field curves for the as-deposited and annealed films recorded at room temperature by using a PPMS system. The obvious hysteresis loops indicate that the samples have room temperature ferromagnetism. As previously described, a series of analysis showed that Co ions are located substitutionally at the Zn sites for the as-deposited and annealed films, and it is reasonable to conclude that the ferromagnetism is intrinsic in our $Zn_{0.92}Co_{0.08}O$ films. For the as-deposited $Zn_{0.92}Co_{0.08}O$ film, the M_s derived from the loop (1) in Fig. 6a is 0.20 ($\pm$0.006) μ_B/Co. After annealed in vacuum and hydrogen atmospheres, it increased to 0.23 ($\pm$0.016) μ_B/Co (loop (3)) and 0.42 ($\pm$0.013) μ_B/Co (loop (4)), respectively. Contrarily, as the film was annealed in oxygen atmosphere, the M_s droped to 0.13 ($\pm$0.016) μ_B/Co as shown in loop (2). These values are within the experimental error arising from uncertainties in the film thickness and instrument sensitivity. Some other research groups have also reported similar annealing effect on the magnetism of oxide DMSs [20, 21]. Fig. 6b shows magnetization curves under field-cooling (FC) and zero-field-cooling (ZFC) conditions with a magnetic field of 7.96×10^4 A/m for the H_2-annealed $Zn_{0.92}Co_{0.08}O$ film. Ferromagnetism behavior can be observed at temperature above 350 K, i.e., curie temperature (T_c) is above 350 K, and it is suitable for the application of room temperature DMS devices.

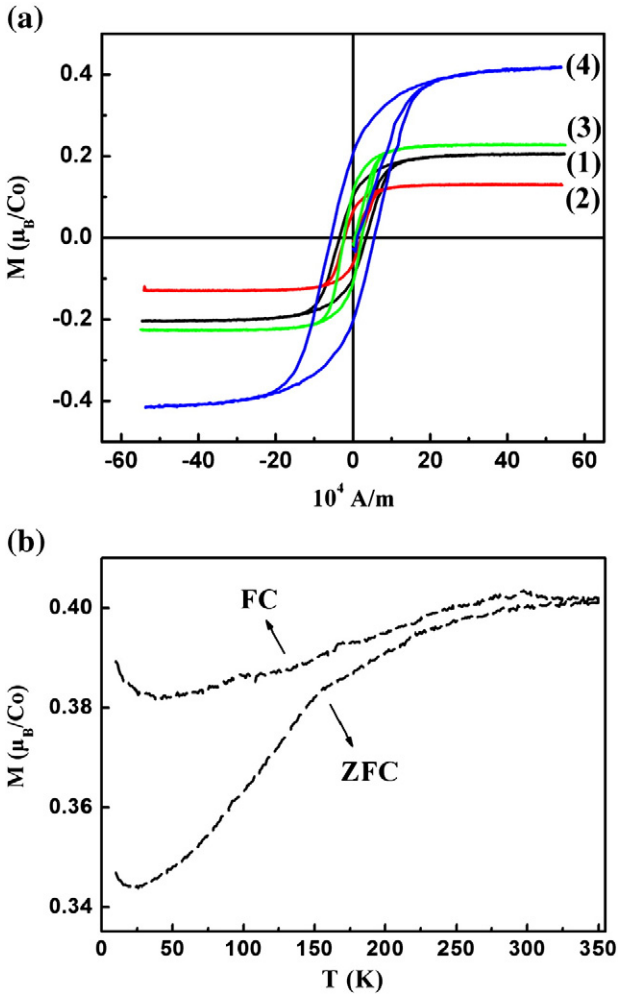

Fig. 6. (a) Magnetic hysteresis loops for $Zn_{0.92}Co_{0.08}O$ thin films recorded at room temperature: (1) as-deposited, (2) O_2-annealed, (3) vacuum-annealed, and (4) H_2-annealed. (b) temperature-dependent magnetization curve of the H_2-annealed sample under field-cooling (FC) and zero-field-cooling (ZFC) conditions.

The room temperature electrical properties of the ZnCoO films were carried out by Hall-effect measurements with a four-point Van der Pauw configuration. It's shown that all of the ZnCoO samples are *n*-type semiconductors. The carrier concentrations of the H_2-annealed and vacuum-annealed ZnCoO films are ~2.46×10^{21} cm^{-3} and ~1.66×10^{20} cm^{-3}, respectively. They are 1–2 orders of magnitude larger than that of the as-deposited films (~7.76×10^{19} cm^{-3}). Nevertheless, the O_2-annealed ZnCoO films exhibit much lower carrier concentration (~2.02×10^{18} cm^{-3}) comparing with the as-deposited films. As it is well known that oxygen vacancies are shallow donors in ZnO materials, at room temperature each oxygen vacancy could contribute to two free electrons and thus results in the increase of carrier (electron) concentration in the ZnO films. As a consequence, the carrier concentration determined by the Hall-effect measurement is directly related to the oxygen density in the ZnO films. In our experiments, the variation of saturated magnetization in terms of annealing environment is well consistent with the trend of carrier (oxygen vacancy) concentrations in the ZnCoO films. This suggests that the oxygen vacancies play an important role in mediating the ferromagnetism in the ZnCoO films, and ultimately a defect-mediated mechanism could be applied to explain the observed room temperature ferromagnetism in our experiments.

4. Conclusion

In summary, uniform $Zn_{0.92}Co_{0.08}O$ DMS thin films with ZnO wurtzite structure have been fabricated on Si (100) and quartz substrates by PLD. The intrinsic ferromagnetism of the $Zn_{0.92}Co_{0.08}O$ thin films is supported by structural and optical measurements. XRD and detailed structural characterizations using x-ray photoemission spectroscopy, UV–visible transmission spectra, x-ray absorption fine structure spectroscopy indicate that Co^{2+} substitute for Zn^{2+} in the tetrahedral configuration without forming secondary phases. The saturated magnetization of $Zn_{0.92}Co_{0.08}O$ films is found to be significantly affected by the annealing atmosphere: oxygen atmosphere annealing weakens the M_s of $Zn_{0.92}Co_{0.08}O$ films while vacuum and hydrogen annealing enhance the M_s. A maximum M_s value of ~$0.42\mu_B$/Co is achieved for the $Zn_{0.92}Co_{0.08}O$ thin film annealed in hydrogen atmosphere. The enhancement of magnetization is possibly due to the increased carrier (electron) concentration that was induced by the generation of oxygen vacancies during annealing in a reducing environment (vacuum and hydrogen), suggesting a mechanism related with carrier-mediated ferromagnetism.

Acknowledgments

This work is supported in part by the National Nature Science Foundation of China (No. 50772032), most of China (No. 2007CB936202), STD and ED of Hubei Province (Nos. 2008BAB010, 2009CDA035, and Z20091001). The authors thank the staff of the XAFS station in NSRL of the University of Science and Technology of China for their assistance in EXAFS measurements.

References

[1] C. Liu, F. Yun, H. Morkoc, J. Mater. Sci. Mater. Electron. 16 (2005) 555.
[2] F. Pan, C. Song, X.J. Liu, Y.C. Yang, F. Zeng, Mater. Sci. Eng. R. 62 (2008) 1.
[3] T. Dietl, H. Ohno, F. Matsukura, J. Cibert, D. Ferrand, Science 287 (2000) 1019.
[4] D.D. Awschalom, M.E. Flatte, Nat. Phys. 3 (2007) 153.
[5] T. Dietl, J. Appl. Phys. 89 (2001) 7437.
[6] R. Janisch, P. Gopal, N.A. Spaldin, J. Phys. Condens. Matter 17 (2005) R657.
[7] S. Ramachandran, Tiwari Ashutosh, J. Narayan, Appl. Phys. Lett. 84 (2004) 5255.
[8] K.R. Kittilstved, D.A. Schwartz, A.C. Tuan, S.M. Heald, S.A. Chambers, D.R. Gamelin, Phys. Rev. Lett. 97 (2006) 037203.
[9] J.M.D. Coey, M. Venkatesan, C.B. Fitzgerald, Nat. Mater. 4 (2005) 173.
[10] Y.X. Wang, X. Ding, Y. Cheng, Y.J. Zhang, L.L. Yang, H.L. Liu, H.G. Fan, Y. Liu, J.H. Yang, Cryst. Res. Technol. 44 (5) (2009) 517.
[11] X.Y. Xu, C.B. Cao, J. Magn. Magn. Mater. 321 (2009) 2216.

[12] Z. Jin, T. Fukumura, M. Kawasaki, K. Ando, H. Saito, T. Sekiguchi, Y.Z. Yoo, M. Murakami, Y. Matsumoto, T. Hasegawa, H. Koinuma, Appl. Phys. Lett. 78 (2001) 3824.
[13] M. Bouloudenine, N. Viart, S. Colis, A. Dinia, Chem. Phys. Lett. 397 (2004) 73.
[14] C.N.R. Rao, F.L. Deepak, J. Mater. Chem. 15 (2005) 573.
[15] Jung H. Park, Min G. Kim, Hyun M. Jang, Sangwoo Ryu, Young M. Kim, Appl. Phys. Lett. 84 (2004) 1338.
[16] J.H. Kim, H. Kim, D. Kim, Y.E. Ihm, W.K. Choo, J. Appl. Phys. 92 (2002) 6066.
[17] K. Sato, H. katyama-Yoshida, Semicon. Sci. Technol. 17 (2002) 367.
[18] J.E. Jaffe, T.C. Droubay, S.A. Chambers, J. Appl. Phys. 97 (2005) 073908.
[19] H.M. Weng, X.P. Yang, J.M. Dong, H. Mizuseki, M. Kawasaki, Y. Kawazoe, Phys. Rev. B 69 (2004) 125219.
[20] N.H. Hong, J. Sakai, N.T. Huong, N. Poirot, A. Ruyter, Phys. Rev. B 72 (2005) 045336.
[21] A. Manivannan, G. Glaspell, P. Dutta, M.S. Seehra, J. Appl. Phys. 97 (2005) 10D325.
[22] H.J. Lee, S.Y. Jeong, C.H. Cho, C.H. Park, Appl. Phys. Lett. 81 (2002) 4020.
[23] J.D. Ye, S.L. Gu, F. Qin, S.M. Zhu, S.M. Liu, X. Zhou, W. Liu, L.Q. Hu, R. Zhang, Y. Shi, Y.D. Zheng, Y.D. Ye, Appl. Phys. A 81 (2005) 809.
[24] P. Koidl, Phys. Rev. B 15 (1977) 2493.
[25] K.J. Kim, Y.R. Park, Appl. Phys. Lett. 81 (2002) 1420.
[26] T.C. Kaspar, T. Droubay, S.M. Heald, P. Nachimuthu, C.M. Wang, V. Shutthanandan, C.A. Johnson, D.R. Gamelin, S.A. Chambers, New J. Phys. 10 (2008) 055010.
[27] S. Yin, M.X. Xu, L. Yang, J.F. Liu, H. Rösner, H. Hahn, H. Gleiter, D. Schild, S. Doyle, T. Liu, T.D. Hu, Phys. Rev. B 73 (2006) 224408.
[28] J.M.D. Coey, A.P. Douvalis, C.B. Fitzgerald, M. Venkatesan, Appl. Phys. Lett. 84 (2004) 1332.
[29] S.A. Chambers, T. Droubay, C.M. Wang, A.S. Lea, R.F.C. Farrow, L. Folks, V. Deline, S. Anders, Appl. Phys. Lett. 82 (2003) 1257.
[30] A. Tiwari, V.M. Bhosle, S. Ramachandran, N. Sudhakar, J. Narayan, S. Budak, A. Gupta, Appl. Phys. Lett. 88 (2006) 142511.
[31] A.C. Tuan, J.D. Bryan, A.B. Pakhomov, V. Shutthanandan, S. Thevuthasan, D.E. McCready, D. Gaspar, M.H. Engelhard, J.W. Rogers Jr., K. Krishnan, D.R. Gamelin, S.A. Chambers, Phys. Rev. B 70 (2004) 054424.
[32] J.T. Prater, S. Ramachandran, A. Tiwari, J. Narayan, J. Electron. Mater. 35 (2006) 852.
[33] B. Huang, D.L. Zhu, X.C. Ma, Appl. Surf. Sci. 253 (2007) 6892.
[34] H. Wang, H.B. Wang, F.J. Yang, Y. Chen, C. Zhang, C.P. Yang, Q. Li, S.P. Wong, Nanotechnology 17 (2006) 4312.
[35] H. Wang, Y. Chen, H.B. Wang, C. Zhang, F.J. Yang, J.X. Duan, C.P. Yang, Y.M. Xu, M.J. Zhou, Q. Li, Appl. Phys. Lett. 90 (2007) 052505.
[36] S. Ramachandran, J. Narayan, J.T. Prater, Appl. Phys. Lett. 88 (2006) 242503.